ARTICLE

Phase Equilibria of Hydrogen Bonding Fluid in a Slit Pore with Broken Symmetry

Xiao-yu Liu[a], Jiang-tao Li[a], Fang Gu[a*], Hai-jun Wang[a,b,c*]

a. College of Chemistry and Environmental Science, Hebei University, Baoding 071002, China
b. Chemical Biology Key Laboratory of Hebei Province, Hebei University, Baoding 071002, China
c. Key Laboratory of Medical Chemistry and Molecular Diagnosis, Ministry of Education, Baoding 071002, China

(Dated: Received on January 4, 2015; Accepted on January 29, 2015)

Phase equilibria of hydrogen bonding (HB) fluid confined in a slit pore with broken symmetry were investigated by the density functional theory incorporated with modified fundamental measure theory, where the symmetry breaking originated from the distinct interactions between fluid molecules and two walls of the slit pore. In terms of adsorption-desorption isotherms and the corresponding grand potentials, phase diagrams of HB fluid under various conditions are presented. Furthermore, through phase coexistences of laying transition and capillary condensation, the effects of HB interaction, pore width, fluid-pore interaction and the broken symmetry on the phase equilibrium properties are addressed. It is shown that these factors can give rise to apparent influences on the phase equilibria of confined HB fluid because of the competition between intermolecular interaction and fluid-pore interaction. Interestingly, a significant influence of broken symmetry of the slit pore is found, and thus the symmetry breaking can provide a new way to regulate the phase behavior of various confined fluids.

Key words: Hydrogen bonding fluid, Broken symmetry, Phase equilibria, Density functional theory

I. INTRODUCTION

In recent years, microporous and mesoporous materials are widely used in fields of physics, chemistry and chemical engineering because of a rapid development of nanotechnology. Physical and chemical properties of the confined fluids such as wetting, phase transition and phase equilibria have attracted intense attentions [1]. As a matter of fact, adsorption properties of nanopore are mainly determined by the geometry of nanopore, fluid-pore interaction and thermodynamic conditions [2, 3]. As is well known, under mesoscopic and microscopic dimensions, fluids would become inhomogeneous and its relevant properties are significantly different from those in the bulk phase. For a pore with various geometries, one can observe the wetting, layering transition (LT) and capillary condensation (CC) [4–6]. Therefore the investigation of phase equilibria of a fluid in a pore can provide some useful clues for designing the related adsorption materials.

In various adsorptions, hydrogen bonding (HB) fluids have shown a rapidly increasing interest because of its characteristic properties [7]. It is well known that, HB fluid is a typical kind of inhomogeneous and multi-scale system, and usually displays very rich phase behavior because various clusters can be formed through hydrogen bonds. In essence, it is hydrogen bonds that result in a significant influence on the aggregated structures and phase properties of HB fluid [8, 9]. In general, the strength of hydrogen bonds and molecular functionality are thought of as the most important factors to characterize HB interaction, where the molecular functionality is referred to the number of proton acceptors and donors of a molecule. Thus one can expect that the two factors can also give rise to similar influences on relevant properties of the confined HB fluid.

In this work the adsorption and desorption isotherms of HB fluid confined in a slit pore with broken symmetry are investigated in terms of the density functional theory (DFT) for classical fluids [10, 11]. Actually, although computer simulations can be selected to study the structure and HBs of fluids such as water between two hydrophobic walls [12], modern liquid theories such as DFT are more computational efficient. An attempt is made to study how the broken symmetry influences the phase behavior of the confined HB fluid. Here the broken symmetry is referred to the interactions between the fluid molecules with two walls of the slit pore different from each other. Experimentally, this kind of bro-

*Authors to whom correspondence should be addressed. E-mail: fanggu@hbu.edu.cn, whj@hbu.edu.cn

ken symmetry can be realized, for instance, when the slit pore is made of two different walls or when one of the two walls is modified by another kind of material. Along this line, some strategies for the synthesis of Janus particle [13] can be used to prepare a slit pore with broken symmetry above-mentioned.

In this work, to reveal the influences of relevant factors on the phase equilibria of HB fluid confined in a slit pore with symmetry breaking, the investigation is performed for HB fluid of A_aD_d type in terms of the DFT for classical fluid, where the symbol A_aD_d denotes a molecule consisting of a proton acceptors and d proton donors. In the calculations, the method of DFT together with the fundamental measure theory (FMT) [14] and modified fundamental measure theory (MFMT) have been used [15, 16]. In detail, the phase equilibria of confined HB fluid are studied by calculating adsorption and desorption isotherms, and then the effect of symmetry breaking, HB interaction and the pore width are presented by means of the corresponding phase diagrams.

II. THEORY

Since the method of DFT for classical fluid was proposed, it has undergone many versions with various approximations. In 1989, the FMT was proposed by Rosenfeld [14] based on the geometry of hard sphere (HS) particle, which recovered the famous 0-dimension results in Percus-Yevick approximation. From then on, FMT and its modified versions [15, 16] have been successfully applied to inhomogeneous fluids and mixtures. So far the DFT approach has shown considerable superiority because of its modest computational cost and higher precision.

The key component of the DFT for classical fluids is constructing the grand potential with the density profile as the functional variable. As the equilibrium density profile is obtained by minimizing the grand potential functional, some physical properties of the fluid can be investigated [10, 11, 13–22]. For a fluid system of interest, the classical DFT states that, the grand potential functional $\Omega[n(\mathbf{r})]$ can be expressed as a functional form by taking the density profile $n(\mathbf{r})$ of fluid as the functional variable, namely

$$\Omega[n(\mathbf{r})] = F[n(\mathbf{r})] + \int [V_{\rm ext}(\mathbf{r}) - \mu] n(\mathbf{r}) \mathrm{d}\mathbf{r} \tag{1}$$

where $F[n(\mathbf{r})]$ is the intrinsic Helmholtz free energy, $V_{\rm ext}(\mathbf{r})$ is the external potential for a single particle and μ is the chemical potential of a particle in the bulk phase.

$F[n(\mathbf{r})]$ can be formally expressed as the sum of an ideal part $F_{\rm id}[n(\mathbf{r})]$ and an excess part $F_{\rm ex}[n(\mathbf{r})]$ by writing

$$F[n(\mathbf{r})] = F_{\rm id}[n(\mathbf{r})] + F_{\rm ex}[n(\mathbf{r})] \tag{2}$$

in which the ideal part $F_{\rm id}[n(\mathbf{r})]$ has been exactly known as,

$$F_{\rm id}[n(\mathbf{r})] = \beta^{-1} \int \{\ln[n(\mathbf{r})\Lambda^3] - 1\} n(\mathbf{r}) \mathrm{d}\mathbf{r} \tag{3}$$

where β^{-1} is the product of Boltzmann constant $k_{\rm B}$ and temperature T, Λ is the thermal wavelength.

The excess part $F_{\rm ex}[n(\mathbf{r})]$ for the present HB fluid under study can be given by

$$F_{\rm ex}[n(\mathbf{r})] = F_{\rm hs}[n(\mathbf{r})] + F_{\rm dis}[n(\mathbf{r})] + F_{\rm hb}[n(\mathbf{r})] \tag{4}$$

where $F_{\rm hs}[n(\mathbf{r})]$, $F_{\rm dis}[n(\mathbf{r})]$ and $F_{\rm hb}[n(\mathbf{r})]$ are the contributions of HS, dispersion and HB interactions, respectively.

Within the framework of FMT and MFMT [14–16], $F_{\rm hs}[n(\mathbf{r})]$ can be expressed as

$$\beta F_{\rm hs}[n(\mathbf{r})] = \int \{\Phi_1[n_\alpha(\mathbf{r})] + \Phi_2[n_\alpha(\mathbf{r})] + \Phi_3[n_\alpha(\mathbf{r})]\} \mathrm{d}\mathbf{r} \tag{5}$$

in which the expressions of $\Phi_1[n_\alpha(\mathbf{r})]$, $\Phi_2[n_\alpha(\mathbf{r})]$ and $\Phi_3[n_\alpha(\mathbf{r})]$ are the following respectively,

$$\Phi_1 = -n_0 \ln(1 - n_3) \tag{6}$$

$$\Phi_2 = \frac{n_1 n_2 - \mathbf{n}_{\rm I} \cdot \mathbf{n}_{\rm II}}{1 - n_3} \tag{7}$$

$$\Phi_3 = \left[n_3 \ln(1 - n_3) + \frac{{n_3}^2}{(1 - n_3)^2} \right] \cdot \frac{{n_2}^3 - 3 n_2 \mathbf{n}_{\rm II} \cdot \mathbf{n}_{\rm II}}{36\pi {n_3}^3} \tag{8}$$

where $n_\alpha(\mathbf{r})$ (α=0, 1, 2, 3, I, II) denote the weighted density and can be derived by means of the weighed function $\omega_\alpha(\mathbf{r} - \mathbf{r}')$, namely

$$n_\alpha(\mathbf{r}) = \int n(\mathbf{r}') \omega_\alpha(\mathbf{r} - \mathbf{r}') \mathrm{d}\mathbf{r}' \tag{9}$$

while the expression of $\omega_\alpha(\mathbf{r} - \mathbf{r}')$ can be found in Ref.[14].

The contribution from dispersion interaction between fluid molecules, under the mean field approximation, can be given by the following expression

$$\beta F_{\rm dis}[n(\mathbf{r})] = \frac{1}{2} \int \int n(\mathbf{r}) V_{\rm dis}(|\mathbf{r} - \mathbf{r}'|) n(\mathbf{r}') \mathrm{d}\mathbf{r} \mathrm{d}\mathbf{r}' \tag{10}$$

in which $V_{\rm dis}(|\mathbf{r} - \mathbf{r}'|)$ denotes the interaction potential between molecules at positions $\mathbf{r}$ and $\mathbf{r}'$. For convenience, in this work $V_{\rm dis}(r)$ will be modeled by a cut-off Lennard-Jones (LJ) potential by using WCA approximation [23]. This means that, there exists a cut-off radius $r_{\rm c}$ to be used such that $V_{\rm dis}(r)$ is zero as $r > r_{\rm c}$ and takes the following form as $r \le r_c$

$$V_{\rm dis}(r) = \begin{cases} -\varepsilon - V_{\rm LJ}(r_{\rm c}), & r < 2^{1/6}\sigma \\ V_{\rm LJ}(r) - V_{\rm LJ}(r_{\rm c}), & 2^{1/6}\sigma \le r \le r_{\rm c} \end{cases} \tag{11}$$

$$V_{\rm LJ}(r) = 4\varepsilon \left[\left(\frac{\sigma}{r}\right)^{12} - \left(\frac{\sigma}{r}\right)^{6} \right] \tag{12}$$

DOI:10.1063/1674-0068/28/cjcp1501001

where the molecular diameter σ denotes the convenient LJ potential with the interaction energy ε.

Furthermore, based on the previous results on an HB fluid of the A_aD_d type, $F_{\rm hb}[n(\mathbf{r})]$ can be written as [24]

$$\beta F_{\rm hb}[n(\mathbf{r})] = \int \{\rho(\mathbf{r}) + n(\mathbf{r}) \ln[(1-p_a(\mathbf{r}))^a \cdot (1-p_d(\mathbf{r}))^d]\} \mathrm{d}\mathbf{r} \quad (13)$$

$$p_a(\mathbf{r}) = \frac{\rho(\mathbf{r})}{a n(\mathbf{r})} \quad (14)$$

$$p_d(\mathbf{r}) = \frac{\rho(\mathbf{r})}{d n(\mathbf{r})} \quad (15)$$

where $\rho(\mathbf{r})$ is the number density of hydrogen bonds at position $\mathbf{r}$, $p_a(\mathbf{r})$ and $p_d(\mathbf{r})$ are the HB degrees of proton acceptors and donors respectively, and they are subject to the following relationship

$$\frac{p_a(\mathbf{r})}{d n(\mathbf{r})[1-p_a(\mathbf{r})][1-p_d(\mathbf{r})]} = \upsilon g_{\rm hs}[n(\mathbf{r})] \cdot [\exp(\beta\varepsilon_{\rm hb}) - 1] \quad (16)$$

here, $\varepsilon_{\rm hb}$ denotes the HB energy, υ is an HB volume parameter, while $g_{\rm hs}[n(\mathbf{r})]$ is the radial distribution function of the HS fluid that can be expressed as [18]

$$g_{\rm hs}[n(\mathbf{r})] = \frac{1}{1-n_3} + \frac{n_2\sigma\xi}{4(1-n_3)^2} + \frac{{n_2}^2\sigma^2\xi}{72(1-n_3)^3} \quad (17)$$

$$\xi = 1 - \frac{\mathbf{n}_{\rm II}\cdot\mathbf{n}_{\rm II}}{{n_2}^2} \quad (18)$$

From Eq.(13), it can be seen that the functional variables of $F_{\rm hb}[n(\mathbf{r})]$ are not only the number density of fluid molecules but also that of hydrogen bonds, and therefore both of them play the key role in characterizing the aggregated structure of the HB fluid. Minimizing the grand potential functional $\Omega[n(\mathbf{r})]$ yields

$$n(\mathbf{r}) = n_{\rm b} \exp\left\{ -\beta \frac{\delta}{\delta n(\mathbf{r})} \{F_{\rm hs}[n(\mathbf{r})] + F_{\rm hb}[n(\mathbf{r})]\} + \beta[\mu_{\rm b} - V_{\rm ext}(\mathbf{r})] \right\} \quad (19)$$

in which $V_{\rm ext}(\mathbf{r})$ denotes the fluid-wall interaction, and $n_{\rm b}$ and $\mu_{\rm b}$ are the bulk density and chemical potential of the HB fluid, respectively. Because of the presence of hydrogen bonds, the bulk chemical potential $\mu_{\rm b}$ can be further expressed as

$$\mu_{\rm b} = \mu_{\rm hs} + \mu_{\rm dis} + \mu_{\rm hb} \quad (20)$$

where $\mu_{\rm hs}$, $\mu_{\rm dis}$ and $\mu_{\rm hb}$ denote the chemical potentials contributed by the HS, dispersion and HB parts with the following forms [25]

$$\beta\mu_{\rm hs} = \frac{\eta}{(1-\eta)^3}(8 - 9\eta + 3\eta^2) \quad (21)$$

$$\beta\mu_{\rm dis} = \frac{32\eta}{3T^*}\left[3\left(\frac{\sigma}{r_c}\right)^6 - \left(\frac{\sigma}{r_c}\right)^9 - 2\right] \quad (22)$$

$$\beta\mu_{\rm hb} = \ln[(1-p_a)^a(1-p_d)^d] - a p_a \frac{\eta(5-2\eta)}{(1-\eta)(2-\eta)} \quad (23)$$

where $\eta = \frac{\pi}{6} n_{\rm b}\sigma^3$ is packing fraction of the bulk HB fluid, and T^* is defined as $T^* = (\beta\varepsilon)^{-1}$. Note that, in the bulk limit, $n(\mathbf{r}) = n_{\rm b}$, $\xi = 1$ and $g_{\rm hs}(\eta) = \frac{1-\eta/2}{(1-\eta)^3}$.

Based on the geometry of slit pore under consideration, one can find that $n(\mathbf{r}) = n(z)$. Furthermore, the symmetry breaking can be characterized by the distinct interaction energies between fluid molecules with two walls of the slit pore. Therefore if H denotes the distance between the two walls, where z is the distance of a molecule from the wall, this kind of broken symmetry can be represented by the following fluid-wall interaction

$$V_{\rm ext}(z) = V(z) + q_{\rm s} V(H - z) \quad (24)$$

where the parameter $q_{\rm s}$ is used to characterize the broken symmetry occurring in the two walls and it ranges from zero to 1. In Eq.(24), the interaction potential $V(z)$ takes the form as [26]:

$$V(z) = \varepsilon_{\rm w}\left[0.4\left(\frac{\sigma}{z}\right)^{10} - \left(\frac{\sigma}{z}\right)^4 - \frac{\sigma^4}{3\Delta\,(z + 0.61\Delta)^3}\right] \quad (25)$$

where $\varepsilon_{\rm w}$ is the fluid-wall interaction energy, and parameters Δ is usually chosen as $\Delta = 0.7071\sigma$.

Note that, for the slit pore without broken symmetry, one can find that the parameter $q_{\rm s}$ should equal to 1. Therefore when $q_{\rm s}$ varies from zero to 1, the effect of symmetry breaking on the properties of HB fluid in the slit pore can be investigated by the change in corresponding equilibrium density profile.

III. RESULTS AND DISCUSSION

A. Calculation details

As mentioned above, the central physical quantity in the framework of DFT is to find the equilibrium density profile of fluid under various conditions. For the present system, Eq.(19) can be solved by the standard Picard method to obtain the equilibrium density profile. During the iteration process, the new and old density profiles are mixed to avoid the divergence according to the following manner

$$n_{\rm in}^{i+1}(z) = f n_{\rm out}^i(z) + (1-f) n_{\rm in}^i(z) \quad (26)$$

where $n_{\rm in}^i(z)$ and $n_{\rm out}^i(z)$ are the input and output density profiles in the i-th iteration step, and f is a mixing parameter and it is adopted as 0.01 in the calculations. The iteration calculations terminate once the maximum difference between the new and old density profiles is smaller than 10^{-6}. The weighted densities and all the integrals in this work are evaluated by a trapezoidal rule with a mesh width equal to 0.01σ. Once the equilibrium

DOI:10.1063/1674-0068/28/cjcp1501001

density profile is obtained, the average fluid density can be given by

$$n_{\rm av} = \frac{1}{H}\int_0^H n(z){\rm d}z \tag{27}$$

At a given temperature, the phase equilibria in a slit pore can be determined according to the requirements satisfied by chemical potential and grand potential for the coexistence phases, namely

$$\Omega[n_{\rm g}(z)] = \Omega[n_{\rm l}(z)] \tag{28}$$

where $n_{\rm g}(z)$ and $n_{\rm l}(z)$ are gas-like and liquid-like density profiles at the equilibrium state, respectively. In general, in order to determine $n_{\rm g}(z)$ and $n_{\rm l}(z)$, one may firstly calculate the grand potential isotherms for adsorption and desorption process and then determines a bulk density at which the adsorption and desorption grand potential isotherms come cross.

Figure 1 shows an example on how to obtain the bulk density from the adsorption and desorption isotherms together with the corresponding grand potential curves, which can be seen in the upper and lower panels, respectively. From the crosspoints in the grand potentials, one can obtain the average densities corresponding to the coexistence phases.

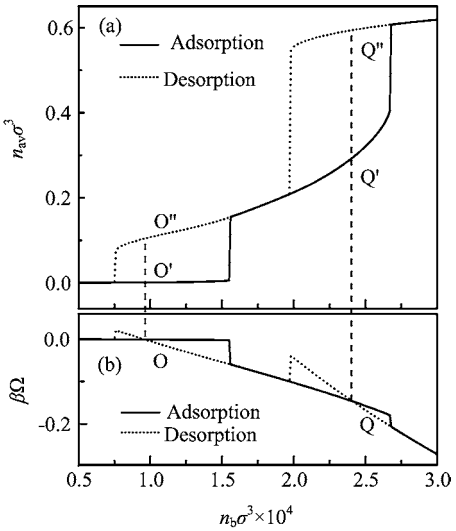

FIG. 1 (a) The adsorption-desorption isotherms and (b) the corresponding grand potential curves from crosspoints O and Q shown in grand potential curves, we can obtain coexistence densities from the points (O′, O″) and (Q′, Q″).

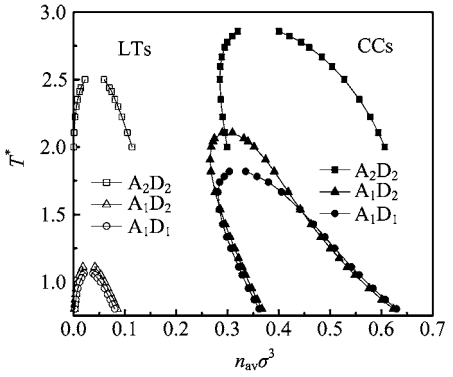

FIG. 2 LTs (open symbol) and CCs (solid symbol) for the confined HB fluid of A_1D_1, A_1D_2 and A_2D_2 types. This phase diagram is obtained under the conditions that $\varepsilon_{\rm hb}/\varepsilon$=20.0, $\varepsilon_{\rm w}/\varepsilon$=15.0, H=7.5σ and $q_{\rm s}$=0.25.

B. The effect of HB interaction on the phase equilibria

For the confined HB fluid, it is obvious that HB interaction is the most important intermolecular interaction, and thus it also gives rise to the corresponding influences on the related properties. In general, upon considering the effect of molecular connectivity, the HB interaction can be considered from two aspects. One is the functionality for forming hydrogen bond, *i.e.*, the number of proton acceptors and proton donors, and another is the HB energy. These two factors should be addressed upon investigating relevant properties of HB fluids.

In this subsection we will turn our attention to how the two factors affect the phase behavior of the confined HB fluid. At first, to learn about the effect of molecular functionality, HB fluids of A_1D_1, A_1D_2 and A_2D_2 types have been taken as examples, which represent the systems of chain-like, branched and network HB fluids, respectively. As a result, we have presented the corresponding phase diagrams under the condition that $\varepsilon_{\rm hb}/\varepsilon$=20.0, $\varepsilon_{\rm w}/\varepsilon$=15.0, pore width H=7.5σ and broken symmetry $q_{\rm s}$=0.25, as shown in Fig.2.

Clearly, there exist LTs and CCs in the phase diagram, in which the left branches represent LTs and the right branches represent CCs. It can be found that, the corresponding critical temperatures rise when the functionality increases and in particular, for the network HB fluid of A_2D_2 type, an increase in its critical temperatures are very significant. Meanwhile, for the network HB fluid, the corresponding phase regions in LT and CC are obviously extended compared with other two types of HB fluids. This is because, in a sense, an increase in functionality means that intermolecular interaction increases, and therefore leads the critical temperatures to rise. In addition, the structure of molecular clusters (chain-like, branched and network structures) may be another factor resulting in the critical temperature to rise.

Furthermore, to reveal the effect of HB energy on the phase behavior of confined HB fluid, we have presented the corresponding phase diagrams of A_2D_2 type fluid in Fig.3 for different HB energies. For easy of presentation, we have used the ratio of HB energy $\varepsilon_{\rm hb}$ to the energy ε of LJ potential as a parameter to study the ef-

DOI:10.1063/1674-0068/28/cjcp1501001

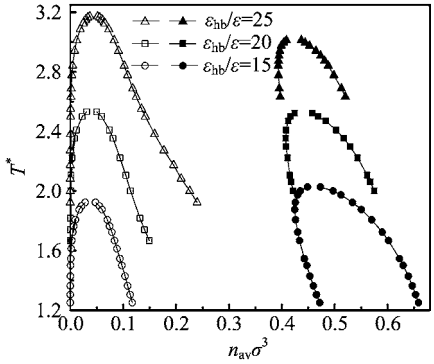

FIG. 3 LTs (open symbol) and CCs (solid symbol) for the confined HB fluid of A_2D_2 types for $\varepsilon_{hb}/\varepsilon$=15.0, 20.0 and 25.0, respectively. This phase diagram is obtained under the conditions that $\varepsilon_w/\varepsilon$=15.0, H=7.5σ and q_s=0.1.

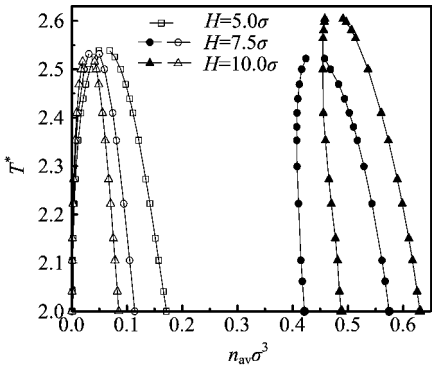

FIG. 4 LTs (open symbol) and CCs (solid symbol) phase diagrams for the confined HB Fluid of A_2D_2 types for H=5.0σ, 7.5σ and 10.0σ, respectively. This phase diagram is obtained under the conditions that $\varepsilon_{hb}/\varepsilon$=20.0, $\varepsilon_w/\varepsilon$=15.0 and q_s=0.1.

fect of HB energy. In obtaining the phase diagram, the conditions that $\varepsilon_w/\varepsilon$=15.0, H=7.5σ and q_s=0.1 have been adopted. It is shown that with an increase in HB energy ($\varepsilon_{hb}/\varepsilon$=15.0, 20.0 and 25.0), the critical temperatures for both LTs and CCs rise significantly and eventually when $\varepsilon_{hb}/\varepsilon$=25.0, the critical temperature of LT has exceeded that of CC. Meanwhile, as the HB energy increases, an obvious increase in the phase regions of LT can be observed. These results mean that the HB energy is indeed a key factor to influence the phase behavior of HB fluid, as expected.

From the above discussions concerning the effect of HB interaction on the phase equilibria of HB fluid, one can conclude that both the functionality and HB energy can result in a significant influence on its phase equilibria. Of course, if what one concerns is beyond the effect of molecular connectivity on the properties of HB fluid, therefore it is necessary that more characters of HB interaction should be taken into account.

C. The effect of pore width on the phase equilibria

For a nano-pore, the pore size is an important parameter to affect the phase behavior of the confined fluid, and in the present system such a parameter is the pore width. Likewise, we can obtain the influence of pore width on the phase equilibria of HB fluid of A_2D_2 type for pore width H=5.0σ, 7.5σ and 10.0σ, respectively. For convenience, the corresponding phase diagram has been calculated under the case that $\varepsilon_{hb}/\varepsilon$=20.0, $\varepsilon_w/\varepsilon$=15.0 and q_s=0.1, as illustrated in Fig.4. Obviously, at a small pore width, only LT in the phase diagram can be observed, and with an increase in the pore width, both LT and CC appear. Meanwhile, with an increase in pore width, the critical temperatures of LTs decrease slightly, but the critical temperatures of CCs increase slightly. In addition, the phase regions of LTs show a shrinking tendency with the pore width increasing.

Interestingly, the tendency of the critical temperature of CC increasing with pore width can be found not only in the confined HB fluid [25], but also in the confined LJ fluid [19, 26] and chain fluid [27]. Therefore, such a phenomenon may be very general and in a sense, it can be considered as a general principle for the confined fluids in nature.

D. The effect of broken symmetry of the slit pore on the phase equilibria

It is our main interest to consider the effect of the broken symmetry on the phase behavior of the confined HB fluids. To this end, we have introduced a broken symmetry parameter q_s to characterize the energy difference between the fluid molecules and two walls of the slit. Seen from Eq.(24), we can know that the situation of slit without broken symmetry corresponds to the case of q_s=1. Therefore the extent of broken symmetry is closely related to the proximity of parameter q_s approaching to zero.

For the HB fluid of A_2D_2 type, upon changing the parameter q_s, one can obtain the corresponding phase diagrams under the conditions that $\varepsilon_{hb}/\varepsilon$=20.0, $\varepsilon_w/\varepsilon$=15.0 and H=7.5σ, as illustrated in Fig.5.

Clearly, a rich phase structure can be observed as q_s varies. First, compared with the case without broken symmetry, the critical temperatures of LT with broken symmetry rise slightly. However, with q_s close to zero, the critical temperature of CC transition rises initially and then lowers. Secondly, with a decrease in parameter q_s, the phase region of CC tends to increase firstly and then decreases. While for the LT, its phase regions always decrease compared with that without broken symmetry. Thirdly, when the symmetry breaking takes place, there is no apparent influence on the critical

DOI:10.1063/1674-0068/28/cjcp1501001

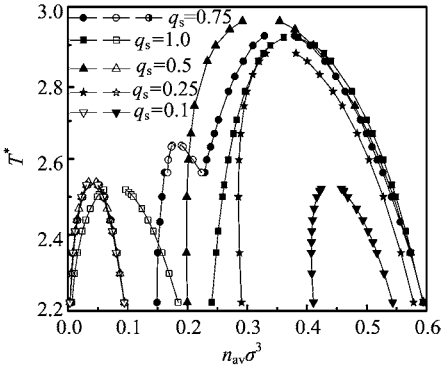

FIG. 5 LTs (open symbol) and CCs (solid symbol) phase diagrams for the confined HB fluid of A_2D_2 types under the case of broken symmetry. This phase diagram is obtained under the conditions that $\varepsilon_{hb}/\varepsilon$=20.0, $\varepsilon_w/\varepsilon$=15.0 and H=7.5σ.

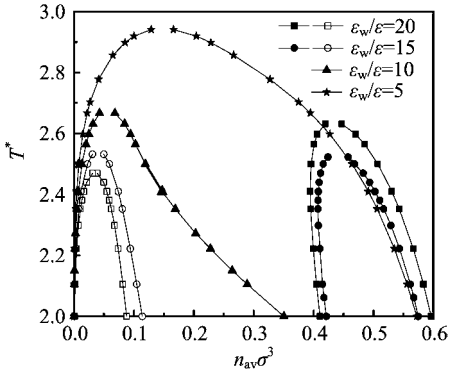

FIG. 6 LTs (open symbol) and CCs (solid symbol) phase diagrams for the confined HB fluid of A_2D_2 types for different fluid-wall interaction under the case of broken symmetry. This phase diagram is obtained under the conditions that $\varepsilon_{hb}/\varepsilon$=20.0, H=7.5σ and q_s=0.1.

temperature and density of LT being found. Interestingly, when q_s=0.75, one can even find that there appears a complicated double-peak structure in the phase diagram of CC. Meanwhile, a broadened density gap under this situation may be found. All these results indicate that the effect of the broken symmetry on the phase behavior of confined HB fluid is very significant, and thus can serve as a new way of regulating phase properties of the confined fluid.

E. The effect of fluid-wall interaction on the phase equilibria

The fluid-wall interaction plays the role of an external field and therefore can be used as an effective factor to regulate the equilibrium density profile of HB fluid, and hence its aggregation state and phase behavior. Likewise, we also use the ratio of fluid-wall interaction energy ε_w to the energy ε as a parameter to characterize the fluid-wall interaction. In so doing, for different values of $\varepsilon_w/\varepsilon$, the corresponding phase diagrams illustrated in Fig.6 enable us to obtain the effect of fluid-wall interaction.

It can be found that, with an increase in the fluid-wall energy, there is an obvious change in the phase behavior of the confined HB fluid. At a relatively low fluid-wall interaction energy, only the gas-liquid like phase transition is observed, and when fluid-wall interaction increases, both the LT and CC take place. Meanwhile, with fluid-wall interaction increasing, the corresponding critical temperatures lower together with phase regions and density gaps shrinking. This is because, when the fluid-wall attraction is relatively weak, the intermolecular interaction dominates and thus leads the LT and CC to vanish. As the fluid-wall interaction becomes strong, the competition between fluid-wall attraction and intermolecular interaction takes place, and as a result, LT and CC are observed.

IV. CONCLUSION

DFT for classical fluids together with FMT and MFMT have been used to investigate the phase equilibria of HB fluid confined in a slit pore with broken symmetry. The corresponding results indicate that phase properties of the confined HB fluid are closely related to the HB interaction and the nature of the slit pore. In essence, the phase behavior of confined HB fluid is determined by the competition between fluid-wall interaction and intermolecular interaction. As a consequence, one can find that, LT and CC sometimes do not take place simultaneously.

As is well known, for the fluid confined in a nano-pore or meso-pore, an apparent fact is that surface or interface effect plays a key role in relevant physical phenomena because of the microscopic or mesoscopic size of the pore. This makes that fluid-wall interaction, intermolecular interaction and geometry of nano-pore become very important. For the HB fluid confined in a slit pore with broken symmetry, their influence of these factors have been investigated. These results are helpful to reveal the phase behavior of confined HB fluid under various geometrical and physical conditions. More importantly, it is found that the symmetry breaking of slit walls could be considered as a new method for regulating the phase behavior of the confined fluid. These factors, depending on the extent of broken symmetry, can lead to a significant effect on the phase region and critical temperature of CC. Therefore compared with the corresponding results without broken symmetry, symmetry breaking occurring in a slit pore can serve as a new way of regulating the phase property of the confined fluids.

It should be noted that, the treatment of HB flu-

DOI:10.1063/1674-0068/28/cjcp1501001

ids in this work is still crude since as an approximation, some important characters such as dipolar interaction, dispersion correlation and non-spherical geometry of fluid molecules have been neglected. Therefore the used model to deal with the HB fluid is very simplified. As is well known, the dispersion correlation plays an important role in improving the mean field approximation, by which an elaborated phase structure can be obtained. In fact, the dispersion contribution can be improved by using a corrected mean field theory [28], perturbative expansion [18, 22], weighted density approximations based on the mean field weighted function [29] and Heaviside step function [30]. In the present work only qualitative features of phase equilibria for the HB fluid in an asymmetric slit pore was investigated, then a simple mean field approximation has been used in the calculation. Clearly, further efforts should be made in order to reveal the phase behavior of confined HB fluid in a deep level.

V. ACKNOWLEDGMENTS

This work was supported by the National Natural Science Foundation of China (No.201374028 and No.21306034), the Natural Science Foundation of Hebei Province (No.B2014201103), and the Natural Science Foundation of Education Committee of Hebei Province (No.QN20131079).

[1] L. J. Dunne and G. Manos, *Adsorption and Phase Behaviour in Nanochannels and Nanotubes*, New York: Springer, 241 (2010).
[2] T. Jozsef, *Adsorption: Theory, Modeling and Analysis*, New York: Marcel Dekker, 175 (2002).
[3] R. Evans, J. Phys.: Condens. Matter **2**, 8989 (1990).
[4] I. A. Hadjiagapiou, Phys. Rev. E **65**, 021605 (2002).
[5] A. V. Neimark, P. I. Ravikovitch, and A. Vishnyakov, Phys. Rev. E **65**, 031505 (2002).
[6] J. Z. Wu, J. Phys. Chem. B **113**, 6813 (2009).
[7] G. A. Jeffrey, *An Introduction to Hydrogen Bonding*, Oxford: Oxford University Press, 135 (1997).
[8] C. Panayiotou and I. C. Sanchez, J. Phys. Chem. **95**, 10090 (1991).
[9] H. J. Wang, F. Gu, X. Z. Hong, and X. W. Ba, Sci. China. Ser. B **50**, 183 (2007).
[10] T. V. Ramakrishnan and M. Yussouff, Phys. Rev. B **19**, 2775 (1979).
[11] R. Evans, *Density Functional in the Theory of Nonuniform Fluids*, In: D. Henderson *Fundamentals of Inhomogeneous Fluids*, New York: Marcel Dekker, 85 (1992).
[12] M. Jia, W. H. Zhao, and L. F. Yuan, Chin. J. Chem. Phys. **27**, 15 (2014).
[13] F. X. Lang, K. Shen, X. Z. Qu, C. L. Zhang, Q. Wang, J. L. Li, J. G. Liu, and Z. Z. Yang, Angew. Chem. Int. Ed. **50**, 2379 (2011).
[14] Y. Rosenfeld, Phys. Rev. Lett. **63**, 980 (1989).
[15] R. Roth, R. Evans, A. Lang, and G. Kahl, J. Phys.: Condens. Matter **14**, 12063 (2002).
[16] Y. X. Yu and J. Z. Wu, J. Chem. Phys. **117**, 10156 (2002).
[17] Z. D. Li, D. P. Cao, and J. Z. Wu, J. Chem. Phys. **122**, 224701 (2005).
[18] D. Fu and X. S. Li, J. Chem. Phys. **125**, 084716 (2006).
[19] B. Peng and Y. X. Yu, J. Phys. Chem. B **112**, 15407 (2008).
[20] P. Tarazona, M. M. T. Dagama, and R. Evans, Mol. Phys. **49**, 283 (1983).
[21] P. Tarazona, U. M. B. Marconi, and R. Evans, Mol. Phys. **60**, 573 (1987).
[22] Y. X. Yu, F. Q. You, Y. P. Tang, G. H. Gao, and Y. G. Li, J. Phys. Chem. B **110**, 334 (2006).
[23] J. D. Weeks, D. Chandler, and H. C. Andersen, J. Chem. Phys. **54**, 5237 (1971).
[24] H. J. Wang, X. Z. Hong, F. Gu, and X. W. Ba, Sci. China. Ser. B **49**, 499 (2006).
[25] F. Gu, H. J. Wang, and D. Fu, Sci. Sin. Chim. **43**, 55 (2013).
[26] D. Fu, J. Chem. Phys. **124**, 164701 (2006).
[27] Y. X. Yu, G. H. Gao, and X. L. Wang, J. Phys. Chem. B **110**, 14418 (2006).
[28] F. Q. You, Y. X. Yu, and G. H. Gao, J. Chem. Phys. **123**, 114705 (2005).
[29] B. Peng and Y. X. Yu, Langmuir, **24**, 12431 (2008).
[30] Y. X. Yu, J. Chem. Phys. **131**, 024704 (2009).

DOI:10.1063/1674-0068/28/cjcp1501001